Int. J. Heat Mass Transfer. Vol. 22, pp. 1355–1374
Pergamon Press Ltd. 1979. Printed in Great Britain

THERMO-FLUID-DYNAMIC EXPERIMENTS WITH GAS-COOLED BUNDLES OF ROUGH RODS AND THEIR EVALUATION WITH THE COMPUTER CODE SAGAPØ

M. DALLE DONNE.† A. MARTELLI‡ and K. REHME
Kernforschungszentrum Karlsruhe, INR, Karlsruhe, West Germany

(*Received* 21 *July* 1978)

Abstract—The paper describes shortly the heat transfer experiments performed with two bundles of 12 and 19 electrically heated rough rods in a high pressure helium loop. The fundamentals of the computer code SAGAPØ are given. SAGAPØ calculates the friction and heat transfer coefficients in turbulent flow by integrating the logarithmic universal law of the wall for velocity and temperature in the various coolant channels confined by rough surfaces. The code accounts for turbulent mixing and cross flow among the channels, for spacer effects on wall temperatures and pressure drop, for fin efficiency effects due to the roughness ribs, and for inlet effects on wall temperatures in case of smooth rods. Also laminar flow can be calculated. The agreement between experiments and computer calculations is very good for turbulent flow. Two further effects, conduction in the rods in the circumferential direction and thermal radiation, have yet to be considered in the code. These two phenomena play an important role for low mass flows and high temperatures.

NOMENCLATURE

A_s, coefficient in the logarithmic velocity profile relative to a smooth surface [dimensionless];

A_t, B_t, coefficients in the logarithmic temperature profile relative to a smooth surface [dimensionless];

B_i, $= \alpha h/k_c$, Biot number [dimensionless];

c_p, specific heat at constant pressure [$\mathrm{W\,s\,kg^{-1}\,K^{-1}}$];

c_t, $= K_{sp}/\varepsilon^2$, modified drag coefficient [dimensionless];

D_h, hydraulic diameter [m];

E_x, $= \dfrac{T_{Wx} - T_B}{T_{W\max} - T_B}$, fin efficiency [dimensionless];

f_i, $= 2\tau_i/(\rho_i u_i^2)$, friction coefficient [dimensionless];

$G(h^+)$, parameter in the logarithmic temperature profile for rough surfaces [dimensionless];

h, height of the roughness ribs [m];

h^+, $= h\rho_h u_h^*/\mu_h = (h/D_h)Re_h\sqrt{f_h/2}$, dimensionless height of the roughness ribs [dimensionless];

h_W^+, $= h\rho_W u_h^*/\mu_W = h/D_h Re_W \sqrt{f_h/2}$, dimensionless height of the roughness ribs evaluated at the wall temperature T_W [dimensionless];

k_c, thermal conductivity of the canning [$\mathrm{W\,m^{-1}\,K^{-1}}$];

k, thermal conductivity of the coolant gas [$\mathrm{W\,m^{-1}\,K^{-1}}$];

K', smooth to total wetted perimeter ratio;

K_1, drag coefficient for the inlet pressure loss [dimensionless];

K_{sp}, drag coefficient for the pressure loss due to the spacer grid [dimensionless];

K_x, $= \dfrac{T_{Wx} - T_B}{T_{W\max} - T_B}$, fin efficiency [dimensionless];

Pr, $= (\mu_B c_{pB})/k_B$, Prandtl number [dimensionless];

Δp, pressure loss [$\mathrm{N\,m^{-2}}$];

r_{in}, inner radius of the canning [m];

r_1, volumetric radius of the rod [m];

r_0, average radius of the $\tau = 0$ line [m];

r_2, average radius of the shroud walls [m];

R_s, roughness coefficient in the logarithmic velocity profile relative to the shroud wall [dimensionless];

$R(h^+)$, parameter in the logarithmic velocity profile for rough surfaces [dimensionless];

$R(h_W^+)_{01}$, $R(h^+)$ value reduced to $T_W/T_b = 1$ and $h/(r_0 - r_1) = 0.01$ [dimensionless];

$R(h_W^+)_{01x}$, $R(h_W^+)_{01}$ value in the region of "fully rough flow", where $R(h_W^+)_{01}$ is quasi constant [dimensionless];

$\Delta R(h^+)$, coefficient in $R(h^+)$ for the transition region between fully rough and hydraulically smooth turbulent flow [dimensionless];

Re, $= (\bar{\rho}\bar{u}D_h)/\bar{\mu}$, Reynolds number [dimensionless];

q, heat power per unit surface, heat flux [$\mathrm{W\,m^{-2}}$];

†Euratom, delegated to the Karlsruhe "Fast Breeder Project", Institute for Neutron Physics and Reactor Engineering.

‡Euratom, delegated to the Karlsruhe "Fast Breeder Project", Institute for Neutron Physics and Reactor Engineering. Now at Comitato Nazionale per l'Energia Nucleare, Bologna, Italy.

St, $= \alpha/(\rho_B u_B c_{pB})$, Stanton number [dimensionless];

t^+, $= \dfrac{(T_{W\infty} - T)\rho_B c_{pB} u_b^*}{q}$, dimensionless gas temperature [dimensionless];

T, temperature of the gas at the considered point [K];

T_b, bulk temperature of the gas in the zone of a flow sector inside the $\tau = 0$ line [K];

T_B, bulk temperature of the gas in a whole flow sector [K];

T_E, gas temperature at bundle inlet [K];

T_{WS}, wall temperature of the shroud [K];

$T_{r_{meas}}$, temperature of the rod wall at the radial position where the thermocouple is placed [K];

T_W, surface rod temperature [K];

$T_{W_{av}}$, surface rod temperature averaged over a roughness rib axial pitch [K];

$T_{W_{max}}$, maximum surface rod temperature over a roughness rib axial pitch [K];

$T_{W\infty}$, surface rod temperature corresponding to an infinite conductivity in the canning [K];

u, gas velocity [ms^{-1}];

$u_b = u_1$, average velocity of the gas in the zone of a flow sector inside the $\tau = 0$ line [ms^{-1}];

u_B, average velocity of the gas in a whole flow sector [ms^{-1}];

u_i, average velocity of the gas in the inner or outer zone (separated by $\tau = 0$ line) of a flow sector (for $i = 1$ or $i = 2$, respectively) [ms^{-1}];

u^+, $= u/u^*$, dimensionless gas velocity [dimensionless];

u_i^*, $= \sqrt{\tau_i/\rho_i}$, friction velocity [ms^{-1}];

y, radial distance from the wall of the considered point in the subchannel cross section [m];

y_i^+, $= \dfrac{\rho_i y u_i^*}{\mu_i}$, dimensionless radial distance from the wall [dimensionless];

y_s, value of y at the shroud surface [m].

Greek symbols

α, convective heat transfer coefficient [$Wm^{-1}K^{-1}$];

ε, blockage factor of the grids [dimensionless];

μ, dynamic viscosity of the gas [$kg\,m^{-1}s^{-1}$];

ρ, density of the gas [$kg\,m^{-3}$];

τ, shear stress at the wall [Nm^{-2}].

Subscripts

av, average;

b, gas physical properties evaluated at the bulk temperature T_b;

B, gas physical properties evaluated at the gas bulk temperature T_B;

c, canning;

E, inlet;

h, hydraulic;

i, average in the zone i ($i = 1$ inside the $\tau = 0$ line, $i = 2$ outside the $\tau = 0$ line);

max, maximum;

meas, measured;

S, shroud; smooth;

sp, spacer;

t, for temperature profile;

T, whole bundle cross section;

W, wall;

∞, infinite conductivity of the canning.

Special signs

$-$, average;

$+$, dimensionless.

1. INTRODUCTION

FOR THE design of Gas Cooled Fast Reactors (GCFR) it is necessary to predict accurately the thermo-fluid-dynamic behaviour of the fuel element bundles. The steady state thermo-fluid-dynamic problem can be described by means of the Navier–Stokes, the continuity and the energy equations. However, the exact solution of these equations at present is impossible, first of all because the flow is turbulent in the normal flow conditions of the reactor and secondly owing to the very complicated geometry of the flow section, the rods (which are artificially roughened in their part where both the temperatures and the heat fluxes are high) and the grid spacers. A third reason for the impossibility of the exact solution of the thermo-fluid-dynamic problem is due to the spacer and inlet effects both on the mass-flow and on the temperature distributions.

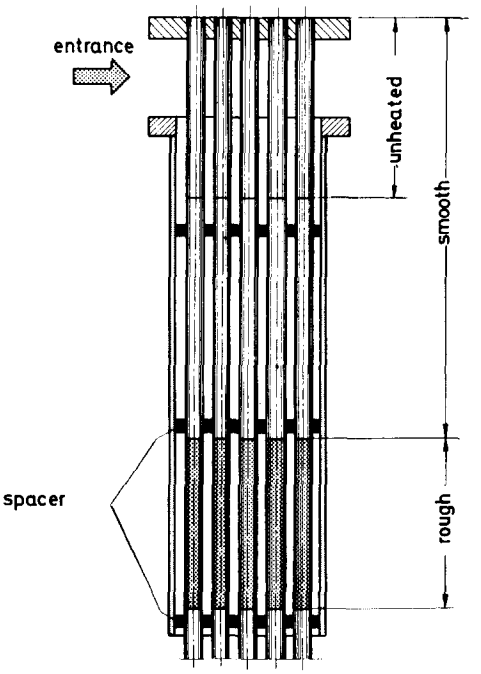

FIG. 1. 19-rod bundle: vertical cross section.

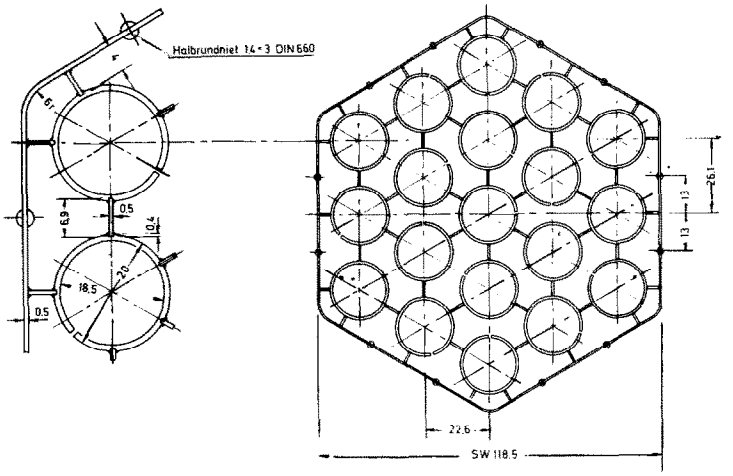

FIG. 2. 19-rod bundle: spacer (dimensions in mm).

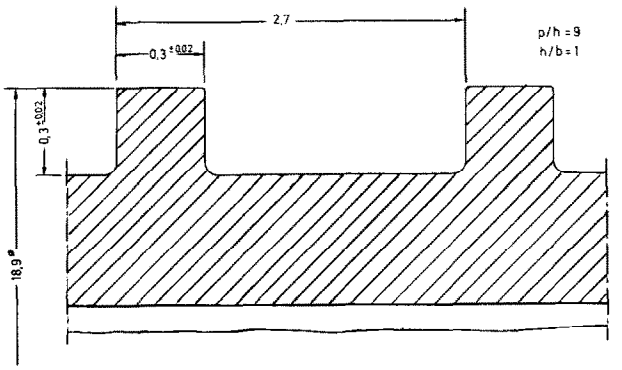

FIG. 3. 19-rod bundle: roughness of the heated rods (dimensions in mm).

Because of the complicated geometry and of the spacer and inlet effects it is impossible to solve the thermo-fluid-dynamic problem exactly, in case of laminar flow also.

Thus it is necessary to develop a computer code which allows a detailed thermo-fluid-dynamic analysis. In such a code the bundle flow section must be finely subdivided and balance equations must be used, which contain terms for the mass, momentum and heat exchange in the transverse directions.

To date no computer code is available which is able to solve the thermo-fluid-dynamic problem with the necessary precision. Therefore we have developed the SAGAPØ-code. We have also performed heat transfer tests on bundles of electrically-heated partly roughened rods (a 19-rod bundle and three 12-rod bundles), which allowed to test the code, this because detailed measurements of temperature distributions in roughened rod bundles similar to GCFR fuel elements were not available to us.

This paper describes shortly the fundamentals of the code SAGAPØ. It also presents comparisons between experimental and computed pressure drop and rod and shroud temperatures for the 19-rod bundle and for a 12-rod bundle (Figs. 1–6).

2. FUNDAMENTALS OF THE SAGAPØ CODE

The physical model and the mathematical procedures used in the code SAGAPØ and the structure of such code have been described in detail in [1–3]. Here only the fundamentals of the code will be shortly presented.†

The mathematical model used in SAGAPØ was initially developed for turbulent flow [4]. Later it was extended to allow the thermo-fluid-dynamic analysis in case of laminar flow as well [1, 5], to test the thermo-fluid-dynamic behaviour of bundles of roughened rods at very low Reynolds numbers.

As usual in thermo-fluid-dynamic codes, the bundle length is subdivided in SAGAPØ into axial sections, in order to approximate the differential equations of continuity, energy and momentum by means of finite difference equations. However, a finer subdivision of the bundle flow sections is possible in SAGAPØ than that normally used in the other codes, both in the case of turbulent flow and of laminar flow. The

†The fundamentals of SAGAPØ have been presented in a previous paper as well [4]. However, at that time, some important effects were not yet considered in SAGAPØ, which are now taken into account.

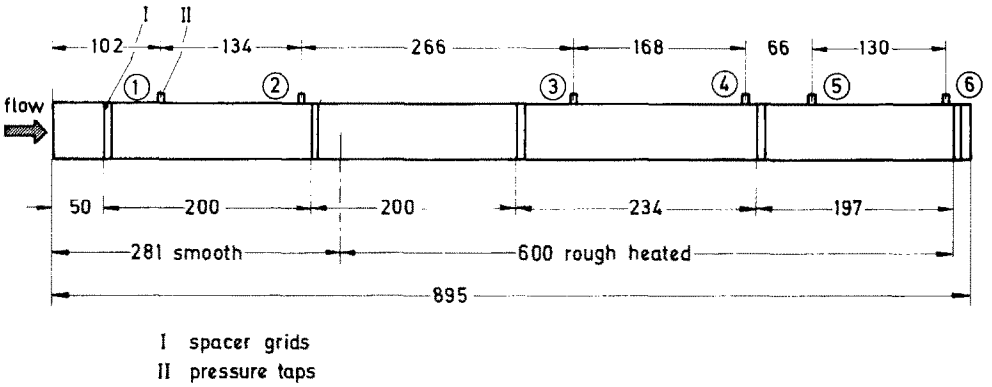

FIG. 4. 12-rod bundle: sketch of the axial geometry (dimensions in mm).

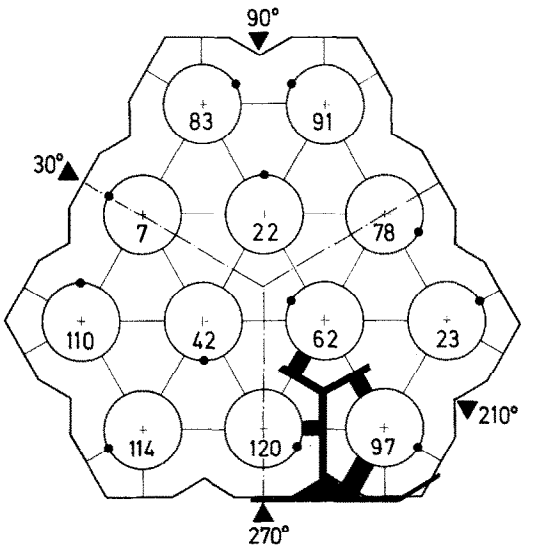

FIG. 5. 12-rod bundle: sketch of flow section and of grid used. The black dots indicate the position of the thermocouples. The numbers are the identification numbers of the rods and the thin straight lines separate the channels used in the SAGAPØ calculations.

reasons for such a fine subdivision which is described below separately for turbulent and laminar flows—depend essentially on the model applied in SAGAPØ for calculating friction factors and Stanton numbers. These reasons are described in detail in [1, 3].

2.1. *Friction factors, Stanton numbers and bundle flow section subdivision*

2.1.1. *Turbulent flow.* In case of turbulent flow it is assumed that the velocity and temperature profiles normal to the rod bundle and shroud surfaces in the cross-sections of the bundle coolant subchannels are given by the logarithmic universal laws of the wall:

$$u^+ = 2.5 \ln \frac{y}{h} + R(h^+) \tag{1}$$

$$t^+ = 2.5 \ln \frac{y}{h} + G(h^+), \tag{2}$$

in case of roughened surfaces, and:

$$u^+ = A_s \ln y^+ + 5.5 \tag{3}$$

$$t^+ = A_t \ln y^+ + B_t, \tag{4}$$

in case of smooth surfaces.

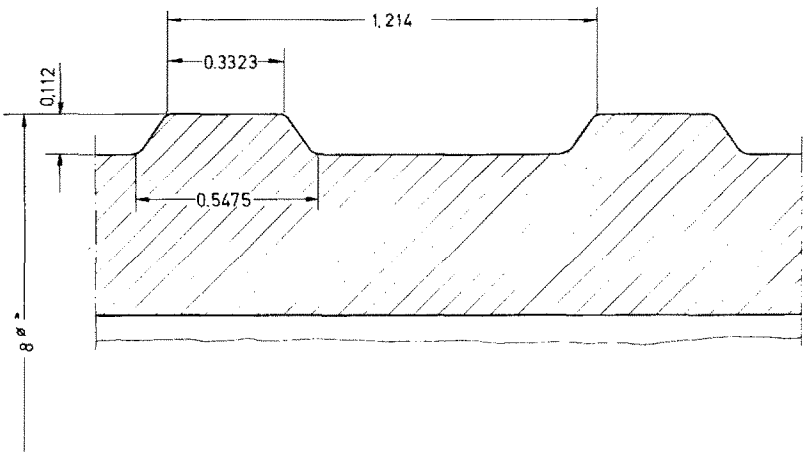

FIG. 6. 12-rod bundle: roughness of the heated rods (dimensions in mm).

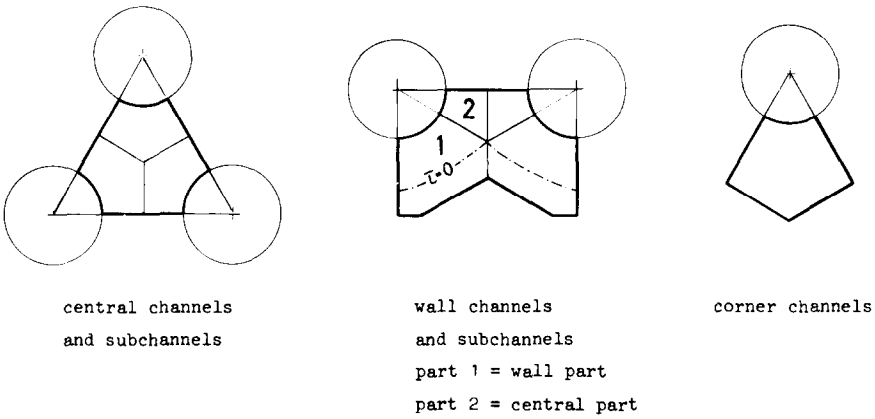

FIG. 7. Division of the flow section into channels and subchannels.

These relationships had been originally established for simpler geometries such as tubes, annuli and parallel plates.

It must be pointed out that in the application of equations (1) and (2) to the rough rod bundle geometry it is implicit that the parameters $R(h^+)$ and $G(h^+)$ and the effect of the determining parameters on them (shape and geometrical parameters characterizing the roughness ribs, cavity Reynolds number h^+ based on the roughness rib height, temperature effects T_W/T_b on $R(h^+)$ and T_W/T_B on $G(h^+)$, length of the velocity and temperature profiles respectively) are considered as invariant in the transformation from the simpler geometries to the bundle [6].

The flow section geometry can be so finely divided that flow regions are defined, which can be considered as perfectly equivalent to sectors of annular sections or to parts of the regions between parellel plates. More precisely, a first division is made into channels of three different types: central channels, wall channels and corner channels (see Fig. 7†).

Each central channel is divided in three subchannels, each wall channel into two subchannels. In the wall subchannels two portions are considered, the separation line of which is the line connecting the center of the rod to the point where the zero stress line ($\tau = 0$ line) intersects the channel symmetry line.

Furthermore it is assumed that the $\tau = 0$ line lies on the symmetry lines separating the three central subchannels for a central channel and on the channel symmetry line for the central portion of a wall subchannel. The position of the $\tau = 0$ line is computed with the method of Dalle Donne [6] in the corner channels and in the wall portion of the wall subchannels.

The zero-heat-flux line ($q = 0$ line) is assumed to lie on the walls of the bundle shroud in the corner channels and in the wall portion of the wall subchannels. In case of heated shroud walls the real position of the $q = 0$ line is not computed, but the real rod and shroud temperatures are evaluated applying the Superposition Principle [1]. In the central subchannels and in the central portion of the wall subchannels it is assumed that the $q = 0$ line is coincident with the $\tau = 0$ line.

Central subchannels, both portions of the wall subchannels and corner channels can be subdivided into sub-subchannels (Fig. 8).† These are defined by means of lines normal to the rod walls in the zones inside the $\tau = 0$ line. In the outer zones the lines are parellel to the channel symmetry lines in the wall subchannels. It must be pointed out that these lines should be normal to the shroud walls to define zones of sub-subchannels which are, similar to flow zones between parallel plates. However, in the case of the 12-rod bundles (see Figs. 5 and 8), it is impossible to define such lines in the whole portion, because, otherwise, a part of the flow section would not be computed. Thus in the wall sub-subchannels of the 12-rod bundles the outer zones are assumed to be equivalent to rectangular flow zones with the same areas as in the real trapezoidal zones (but the equivalent diameters are evaluated by means of the real wetted perimeters). In the corner channels there is a first step in the calculation of the sub-subchannels, where the lines are assumed as normal to the shroud walls in the outer zones, to follow the direction of the velocity profiles; but, this way, a small part of the channel is not computed. Then a second calculation is performed, where the $\tau = 0$ line is assumed to lie at the same position as computed in

†Figure 7 refers to the shroud geometry of the twelve-rod bundle (angular corner channels, blocking triangles with straight sides and base angles of 30° in the wall channels). The shape of the shroud of the nineteen-rod bundle is obtained taking the height of the blocking triangles equal to zero. For different shroud profiles (for example with round corner channels), "equivalent" corner and wall channels of the type shown in Fig. 7, with the real area, and correction factors for the wetted perimeters of such equivalent channels are assumed (see [3]).

†The subdivision into sub-subchannels is normally not needed in case of central and corner channels, if only the calculation of average subchannel rod temperatures is required and not that of the circumferential temperature profiles along the rod perimeter (see [3]). On the contrary, in case of wall subchannels, a fine sub-subchannel subdivision is essential, to assess the position of the line which separates the two portions with the necessary precision [1, 3].

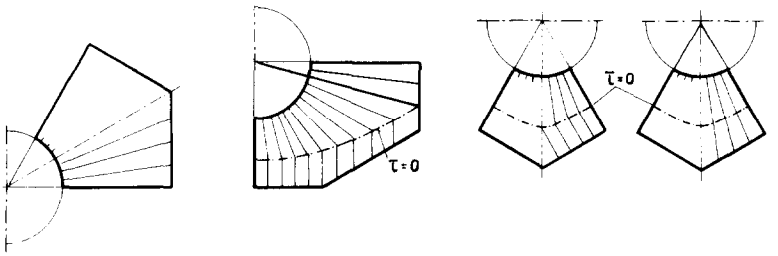

FIG. 8. Subdivision into sub-subchannels.

the first step and the sub-subchannels are defined by means of lines normal to the rod walls, in the outer zones also, to follow the direction of the temperature profiles.

The preceding definition of the sub-subchannels allows the use of the equations derived by the integration of the logarithmic velocity and temperature profiles obtained for annular flow sections and parallel plates: the zone of the sub-subchannels inside the $\tau = 0$ line can be considered to be the inner zone of a section of an annulus; the outer zone is assumed to be a section of one of the two zones between parallel plates (only in the second calculation step of the corner sub-subchannels the outer zone is considered to be a section of the outer zone of an annulus).

In the case of the roughened rods, the friction factors and the surface temperatures are obtained by integrating the velocity and temperature profiles [equations (1) and (2)] in the sub-subchannels. The friction factors in the outer flow zones (relative to the shroud walls) of the sub-subchannels of the wall and corner channels facing the rough rods are also calculated by integration of the logarithmic velocity profile normal to the shroud surface:

$$u^+ = A_s \ln y^+ + 5.5 R_s, \tag{5}$$

whereby:

The slope A_s of the logarithmic profile is taken as a function of the friction factor of the facing rough rod, as explained in [6] (if the facing rod is smooth, then A_s is set equal to 2.5 as in the case of turbulent flow in smooth tubes [7]);

R_s is a parameter taking into account the roughness of the shroud walls ($R_s = 1$ for smooth walls and $R_s < 1$ for rough walls).

By these integrations the average values $\bar{u}^+$ and $\bar{t}^+$ of these profiles are obtained. These average values are directly correlated to the friction factors and Stanton numbers by the expressions:

$$\bar{u}_i^+ = \sqrt{2/f_i} \tag{6}$$

$$\bar{t}_B^+ = \frac{\sqrt{f_1/2}}{St_B} \frac{u_1}{u_B}, \tag{7}$$

where $i = 1$ for flow zones inside $\tau = 0$, $i = 2$ for flow zones outside $\tau = 0$; B refers to the whole flow zone, $1+2$.

The surface temperatures of the shroud wall facing the rough rods are obtained directly from the temperature profile of equation (2), writing (2) at the shroud position y_S.

The mentioned equations do not contain any adjustable coefficients: the computed friction factors and rod and shroud temperatures differ, for the different flow zones, only because of the different geometries, velocities and temperatures.

In the case of smooth rods, the friction factors are also computed by integration of the logarithmic velocity profile, in a way similar to that previously described for roughened rods,† while the rod and the shroud temperatures are evaluated directly with the general equations suggested by Petukhov and Roizen for annular flow sections [8] and corrected for the temperature effect due to the gas property variations with temperature in a channel cross section normal to the flow $((T_W/T_E)^{-c}$ as suggested by Dalle Donne and Meerwald [9] or $(T_W/T_B)^{-c}$, c being an input parameter, the value of which depends on the nature of the gas coolant [3]).

Thus, in this case, no direct use is made of the temperature profiles for calculating rod and shroud temperatures.‡

It must be pointed out that general equations would be too complicated for cooling channels around both smooth and rough surfaces, due to the complicated influence of the roughness parameters.

Both in case of roughened and smooth walls, the subchannel friction factors and rod and shroud temperatures are obtained combining the sub-subchannel values. In a similar way, by combination of the subchannel values, the friction factors of the

†For smooth rods the velocity profiles are given by equation (3) with $A_s = 2.5$, as previously pointed out, and $R_s = 1$, for the profiles relative to the rod walls.

‡However, an integration procedure of the temperature profiles is used in case of smooth rods also, for the calculation of the bulk temperatures of two zones separated by the $\tau = 0$ line, which slightly affect the friction factors [1, 9].

channels and that of the whole bundle flow section are evaluated.

2.1.2. *Laminar flow.* In case of laminar flow no use is made in SAGAPØ of velocity and temperature profiles for calculating friction factors and rod and shroud temperatures. Instead theoretical equations are used for their evaluation. Since these equations, partly derived approximating tabulated analytical results available in the literature (see Refs. [1, 10–12]), are valid for the *entire* corner channels, central subchannels and portions of wall subchannels, the sub-subchannel analysis is not performed.

2.2. *Continuity, energy and axial momentum equations*

The continuity, energy and axial momentum equations for the flow zones previously defined (whole bundle flow section, channels, subchannels, portions of wall subchannels and sub-subchannels) are evaluated by means of balances on each axial section. In the model applied in the SAGAPØ code each channel interacts with the adjacent ones, as usually assumed in the most advanced thermo-fluid-dynamic codes. The further subdivision of channels into subchannels allows to compute different values for mass-flow rate and bulk temperature around the single rods bounding each channel. In order to limit the calculation time, SAGAPØ assumes that each subchannel of a channel interacts with the other subchannels of the same channel and with the channels adjacent to it (a subchannel is adjacent to two channels). Thus, as soon as the channel calculation is performed, the subchannel mass flow rates and temperatures can be computed *separately* for each channel, since the variables for the adjacent channels are already known and the knowledge of those for their subchannels is not needed. A similar simplification is made for the two portions of the wall subchannels (the definition of which is necessary because a whole wall subchannel cannot be considered as equivalent to an annular sector [1]): the mass flow rates and bulk temperatures of the two portions are computed *separately* for each wall subchannel, as soon as the subchannel calculation is performed, under the assumption that each portion interacts with the other portion of the same wall subchannel, with the other subchannel of the same wall channel and with its adjacent channel (a portion of wall subchannel is adjacent to only one channel). The procedure used for the sub-subchannels is further simplified and will be shortly described below.

The interaction terms between adjacent flow zones, which are taken into account in SAGAPØ, are the following:

1. Turbulent mixing (in case of turbulent flow);
2. Cross-flow;
3. Transverse conduction within the gas.

Obviously turbulent mixing does not lead to any redistribution of the mass-flow. However, it causes a redistribution of momentum and enthalpy, if the velocities and the temperatures are not equal in the adjacent flow zones. The effect of turbulent mixing between channels has been taken into account in the code with the method of Kjellström [13], using the mixing coefficients of Ingesson and Hedberg [14], corrected as suggested by Stiefel [15] (correction coefficient equal to 0.5 for the 19 and the 12 rod bundles). The Kjellström method has been also applied for evaluating the turbulent mixing exchange between the subchannels of each channel and between the two portions of each wall subchannel, but assuming, in this case, mixing coefficient values equal to one. This was done because, failing the gap at the boundaries between these flow zones, the transverse velocity and temperature profiles do not present any peak at these boundaries.†

Due to cross-flow a net redistribution of the mass flow occurs. This can be understood considering that in case of gas cooled bundles the transverse pressure gradients are very small (they are neglected in SAGAPØ). Without a net mass flow redistribution, in case of different velocity and/or friction, and/or spacer blockage, and/or heating, the pressure would be different in adjacent flow zones: thus, there must be a net mass-flow redistribution, which eliminates the transverse pressure gradients. The cross-flow is then directed from the zones where, in case of no cross-flow, the axial pressure drop would be higher to those where it would be lower.

The assumption of no pressure gradients in the transverse directions, together with that of appropriate average values for cross-flow velocities and temperatures, allows neglecting the transverse momentum equations (see [1]).

The third mentioned interaction term, conduction within the gas, is obviously present only in the energy equations. It is of importance only in case of low Reynolds numbers.

The mentioned interaction terms are taken into account *explicitly* for the calculation of the mass-flow rate and temperature distributions of channels, subchannels and portions of wall subchannels. On the contrary, for the sub-subchannel calculation (performed only in case of turbulent flow), in order to simplify the mathematical model and thus to avoid unbearably high calculation times, the contributions of the transverse interactions to energy and axial momentum equations are assumed to be *uniform* for all sub-subchannels of the same subchannel or portions of wall subchannels. Thus these terms can be evaluated iteratively in a simple way. A detailed discussion about this procedure is presented in [1].

From the above considerations it is evident that a rather complicated iterative procedure is applied in SAGAPØ to solve the balance equations. Schematically the procedure is, for each axial section, the following:

†For a more detailed discussion of this topic see [3].

1. An initial value is assumed for the whole bundle friction factor f_T;
2. The axial section pressure drop is computed, which corresponds to the current value of f_T, by applying the balance equations to the whole bundle flow section:
3. The friction factors of sub-subchannels are computed, and, from their combination, the corresponding subchannel and channel values are evaluated;
4. The channel calculation is performed;
5. The subchannel calculation is performed;
6. The calculation for the two portions of each wall subchannel is carried out;
7. A new value of f_T is computed and the procedure above is repeated until convergence is reached.

Finally it must be pointed out that in the most recent version of SAGAPØ [3] the calculation of the subchannels and that of the two portions of the wall subchannels has been made optional to allow less accurate but faster calculations.

2.3. *Other features of SAGAPØ*

With SAGAPØ it is possible to consider smooth and roughened rod surfaces. The shroud walls can also be considered as rough [1, 4].

Inlet and spacer effects on pressure drop and on heat transfer are taken into account, in the cases where correlations or at least enough theoretical or experimental data were available at the time at which SAGAPØ has been developed. More precisely the following effects have been considered:

(a) The pressure losses at the spacer grids are taken into account with a method suggested by Rehme [16];
(b) The influence of the spacers on the wall temperature of the rods is evaluated with equations obtained from experiments of Marek and Rehme [17];
(c) The inlet effects on pressure drop and rod and shroud wall temperatures in case of laminar flow are calculated with equations which approximate tabulated theoretical results available in the literature for pressure [18] and temperature distributions in annuli [19];
(d) The inlet effect on rod wall temperatures in case of turbulent flow and smooth rods is calculated with the equations of Petukhov and Roizen [8].

The code computes isothermal flows as well as mass flow and temperature distributions in case of flow with heat transfer. The rods can be equally or unequally heated. The shroud can be heated or unheated. A constant or a not constant power profile in the rods and in the shroud can be considered.

Some corrections are applied in the code. The most important one refers to the so-called "fin efficiency effect". This effect derives from the fact that the local heat transfer coefficient between a roughened rod surface and the cooling gas is not constant in the region between two roughness ribs and on the ribs themselves, and that the thermal conductivity of the gas is not negligible with respect to that of the cladding material [20–22]. The fin efficiency effect depends on the geometry parameters defining the roughness, on the dimensionless group $B_i = \alpha h/k_c$, known as the Biot number, as well as on the thickness of the cladding, on the distribution of the heat transfer coefficient and on the distribution of heat input, and may be expressed in terms of E_∞ and K_∞ as defined by the following equations:

$$E_\infty = (T_{W\infty} - T_B)/(T_{W_{max}} - T_B) \tag{8}$$

$$H_\infty = (T_{W\infty} - T_B)/(T_{W_{av}} - T_B). \tag{9}$$

Another correction is possible if it is necessary to make a comparison between computed and measured rod temperatures, and the thermocouples do not measure the surface temperatures, but are placed within the thickness of the rod walls. In case of electrically-heated tubes, as in the tests for the nineteen- and the twelve-rod bundles described in this work, the correction is performed by means of the following equation:

$$\int_{T_{meas}}^{T_{W_{av}}} k_c(T)\,dT = \frac{qr_1}{r_1^2 - r_{in}^2}\left(\frac{r_1^2 - r_{meas}^2}{2} + r_{in}^2 \ln\frac{r_{meas}}{r_1}\right), \tag{10}$$

which takes into account the radial heat conduction in the tube walls.

Finally, SAGAPØ is able to correct the input dimensions to take into account the thermal expansion of the structure.

To date, heat conduction in the rods both in the axial and in the azimuthal directions, heat radiation and natural convection are not considered in SAGAPØ. Especially azimuthal conduction and heat radiation are of importance in case of laminar flow [23]. They will be introduced in SAGAPØ as soon as possible.

3. COMPARISON BETWEEN COMPUTED AND EXPERIMENTAL RESULTS

The methods described above were used for the evaluation of the experiments with two bundles of electrically heated nineteen and twelve rough rods respectively. These experiments have been carried out in the Helium High Pressure Loop of the Institute of Neutron Physics and Reactor Engineering of the Karlsruhe Nuclear Center. The results of these experiments and a description of the experimental apparatus and experimental techniques used are given in [4, 24, 25]. Here we will present only a comparison of these experimental results with the computations performed with SAGAPØ.

3.1. *Comparison between computed and experimental results for the* 19*-rod bundle*

The experiments covered a Reynolds number range between $Re_E = 1.1 \times 10^3$ and $Re_E = 1.1 \times 10^5$, Re_E being the Reynolds number at the bundle inlet.

The maximum rod linear power achieved was 116 W cm^{-1}, resulting in a maximum heat flux of 20 W cm^{-2}. The maximum measured wall temperature was 880°C. The experimental results are contained in [24]. The comparison between the experimental and the computed results for the turbulent thermal tests (tests 1–3, 8–11) and for a laminar test (test 4) are presented in Reference [1].† In this reference some effects are also accurately described, which probably affect the measurements (as bowing of some rods, natural hydraulic roughness of the shrouds, etc.).

In the present paper the comparison between experiments and calculation is presented only for a turbulent test (test 1 of [1]). No comparison for laminar flow tests is given here, because there are still uncertainties on the accuracy of the measurements at low flow and because SAGAPØ does not consider yet circumferential thermal conduction and thermal radiation among the rods and among shroud and rods, which play an important role in the tests at low flow and high temperature (see [23]).

Dalle Donne and Meyer, on the basis of their experimental results and of a large amount of data from the literature, were able to establish a general correlation for the friction and heat transfer data of surfaces roughened with two-dimensional rectangular ribs [26]. With this correlation, the $R(h^+)$ and $G(h^+)$ parameters for the roughness used in the nineteen-rod bundle (two-dimensional rectangular ribs with $p/h = 9$, $h/b = 1$) are given by the relationships (in case of coolants like air and helium):‡

$$R(h^+) = 2.71 + \Delta R(h^+) + 0.4 \ln\left(\frac{h}{0.01(r_0 - r_1)}\right) + \frac{5}{\sqrt{h_W^+}}\left(\frac{T_{W\infty}}{T_b} - 1\right)^2 \quad (11)$$

$$G(h^+) = 3.81 (h_W^+)^{0.274} Pr^{0.44} \left(\frac{T_{W\infty}}{T_B}\right)^{0.5} \times \left(\frac{h}{0.01(r_2 - r_1)}\right)^{0.053} \quad (12)$$

The only uncertainty of the correlation proposed by Dalle Donne and Meyer in [26] refers to the term $\Delta R(h^+)$, which takes into account the variation of $R(h^+)$ in the transition region between fully rough flow regime (where $\Delta R(h^+) \approx 0$) and turbulent hydraulically smooth flow regime. For the SAGAPØ calculations of [1], since specific experimental results at low h_W^+ values were not available yet for the rods of the nineteen-rod bundle, it was assumed:

$$\Delta R(h^+) = \frac{5100}{(h_W^+)^3}, \quad (13)$$

as suggested in [26] on the base of experimental results for isothermal tests performed for a rough rod different from the rods of the nineteen-rod bundle. However, since the subchannel values of h_W^+ were high enough in the calculations of [1] ($h_W^+ > 20$), it was really not very important, for these calculations, to make use of an accurate equation for $\Delta R(h^+)$. Recent experiments for one single rod of the nineteen-rod bundle tested in an annulus [27] have shown that the $\Delta R(h^+)$ function depends strongly on the roughness geometry and, furthermore, the equation to be used in case of the thermal tests is different from that valid for the isothermal ones (the transition with isothermal flow is more rapid with decreasing flow velocities, i.e. the negative exponent of h_W^+ is higher). In fact, in presence of heat transfer, the following equation must be used for the nineteen-rod bundle:

$$\Delta R(h^+) = \frac{10.84}{h_W^+}, \quad (14)$$

(see Fig. 17 in [27]), which at low h_W^+ values gives considerably smaller $R(h^+)$ values than those derived from equation (13). For the h_W^+ values of the thermal tests investigated in [1], and especially for test 1 ($h_W^+ = 150 \div 190$), the results of which are presented here, the effects due to the use of equation (14) in place of equation (13) are small (about 2% error for $R(h^+)$ in test 1).

In the SAGAPØ calculations uniform inlet mass flow and temperature distributions were assumed. Figure 9 shows a comparison between measured and computed pressure drop for test 1. The shroud walls were assumed to be hydraulically smooth (i.e. $R_s = 1$; see [1]). The coefficient K_E for the inlet pressure loss:

$$\Delta p_E = -K_E \frac{\rho_B u_B^2}{2}, \quad (15)$$

was assumed equal to 1.2 for all tests, which is an acceptable value for a rod bundle.†

The pressure losses due to spacer grids (there are spacers in the smooth part of the bundles only, in case of the nineteen-rod bundle) were computed according to the correlation suggested in [16] as:

$$\Delta p_{sp} = -c_v \varepsilon^2 \frac{\rho_B u_B^2}{2}. \quad (16)$$

The function $c_v = c_v(Re)$ was not directly measured in the Water Loop of the Institute of Neutron

†In [1] the comparison is not shown for tests 5 and 6 for which the flow is in the transition region between laminar and turbulent conditions: equations were not available at the time of the calculations for this Re-range.

‡In case of other gases (for instance CO_2 or steam) the exponent of the temperature correction factors in equations (11) and (12) could be quite different, due to the different variations with temperature of the relevant gas physical properties in the considered flow cross-section.

†Beside the assumption on the shroud roughness parameter R_s (reasonable because of the type of the shroud surface), this is the only other assumption, not substantiated by experimental data, performed in the calculations. This assumption was necessary, because the inlet pressure drop could not be directly measured. The same value for K_E has been assumed for the twelve-rod bundle as well.

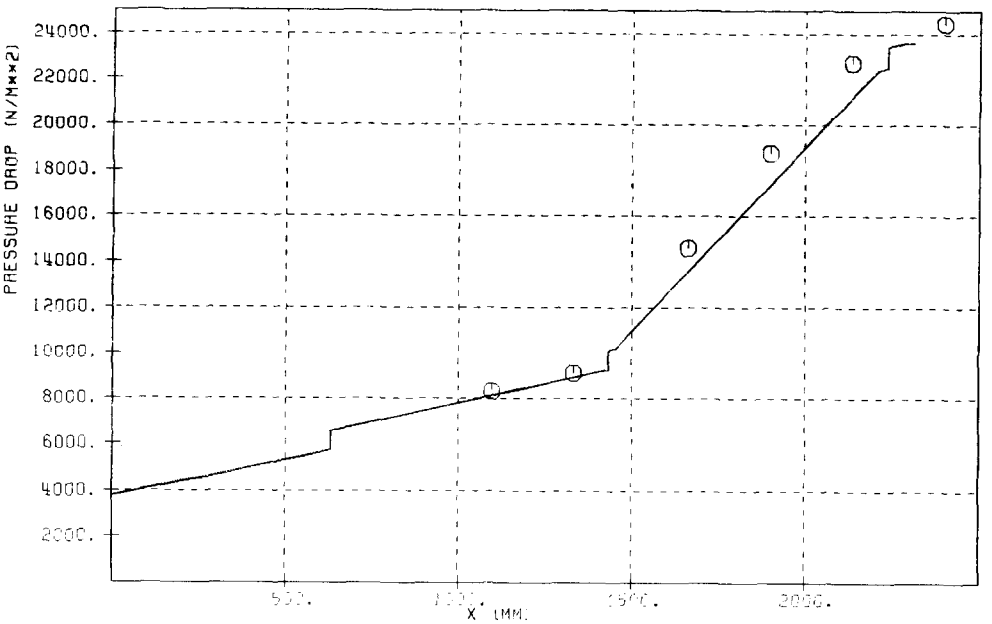

FIG. 9. Comparison between calculated and measured pressure drop in the 19-rod bundle by turbulent flow ($Re_L = 1.12 \times 10^5$).

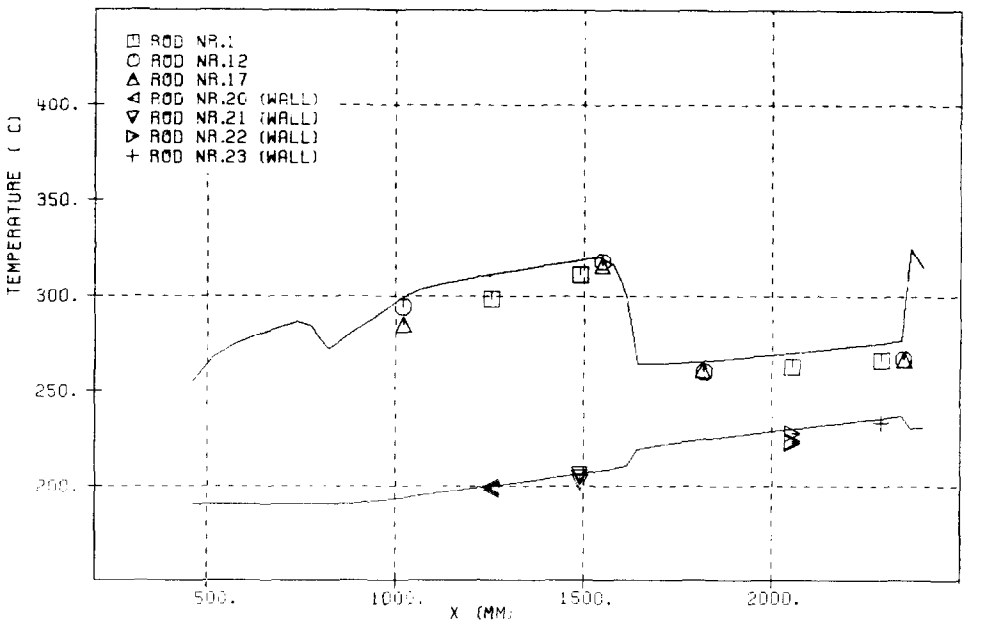

FIG. 10. Comparison between calculated and measured temperatures of the rods and of the shroud wall in the corner channels (19-rod bundle, turbulent flow: $Re_E = 1.12 \times 10^5$).

Physics and Reactor Engineering (contrary to the case of the grids for the 12-rod bundle), thus c_v had to be derived from the values available for similar grids [16]. For the performed turbulent calculations ($Re > 4 \times 10^4$) a constant value of $c_v = 6.5$ was assumed as suggested in [16]. No pressure recovery was assumed at the bundle outlet. It can be concluded that the agreement between the measured and the computed pressure losses is good, especially if one remembers that no adjustable factors were introduced in the calculations (the maximum difference between computed and measured pressure drop for all tests reported in [1] is $\sim 8\%$).

Figures 10–16 show the measured and computed rod and shroud temperatures in the various subchannels (the position of the thermocouples is indicated in the figures). Some remarks are necessary about the calculations:

(a) Due to the relatively low heat flux ($\leqslant 20\,\mathrm{W\,cm^{-2}}$) it has been found that the correction given by the parameter E_∞, and due to fin efficiency effect,

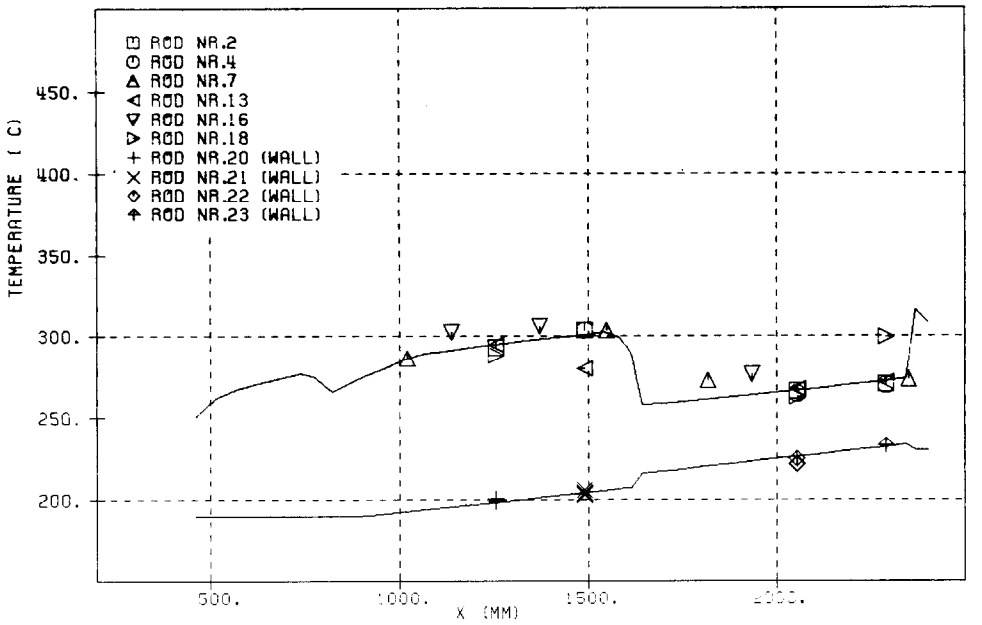

FIG. 11. Comparison between calculated and measured temperatures of the rods and of the shroud wall at the intersection between two wall channels (19-rod bundle, turbulent flow: $Re_E = 1.12 \times 10^5$).

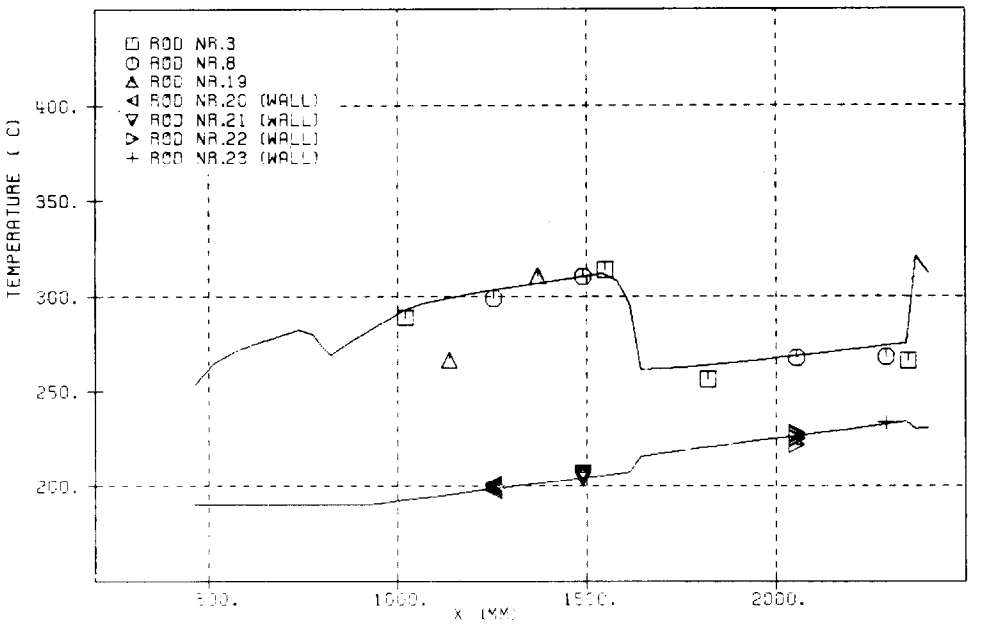

FIG. 12. Comparison between calculated and measured rod temperatures at the intersection between a corner and wall channel and of the shroud temperatures in a wall channel (19-rod bundle, turbulent flow: $Re_E = 1.12 \times 10^5$).

is very small in the case of the 19-rod bundle [1]. As a result of this and because no equation is available for the evaluation of the fin efficiency parameter K_∞ (the use of which is more reasonable to correct the surface rod temperature than that of E_∞, because in the 19-rod bundle the thermocouples, due to their relatively large size, tend to give the average temperature value between the two ribs and not the maximum, although they are placed in the middle between two ribs), the "fin efficiency effect" has been neglected for the 19-rod bundle;

(b) No correction has been performed to take into account the position of the thermocouple inside the canning walls, because this correction is small and because the thermocouples are not all set at the same radial position, some of them being closer to the rod surface and some more inside the cladding wall;

(c) The temperature factor for the correction of

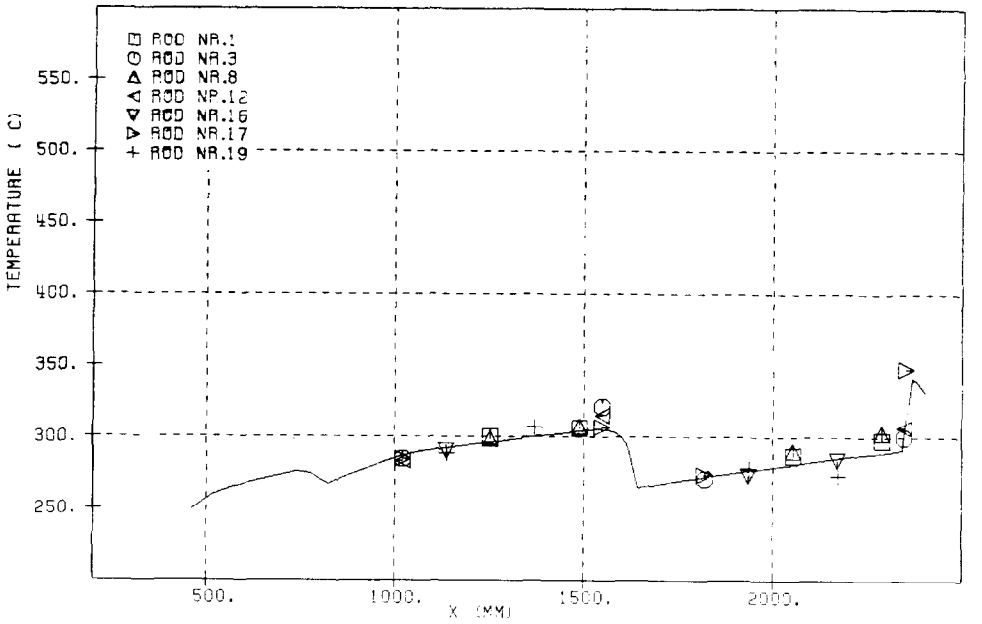

FIG. 13. Comparison between calculated and measured rod temperatures in the central subchannels relative to the outer row of rods (19-rod bundle, turbulent flow: $Re_E = 1.12 \times 10^5$).

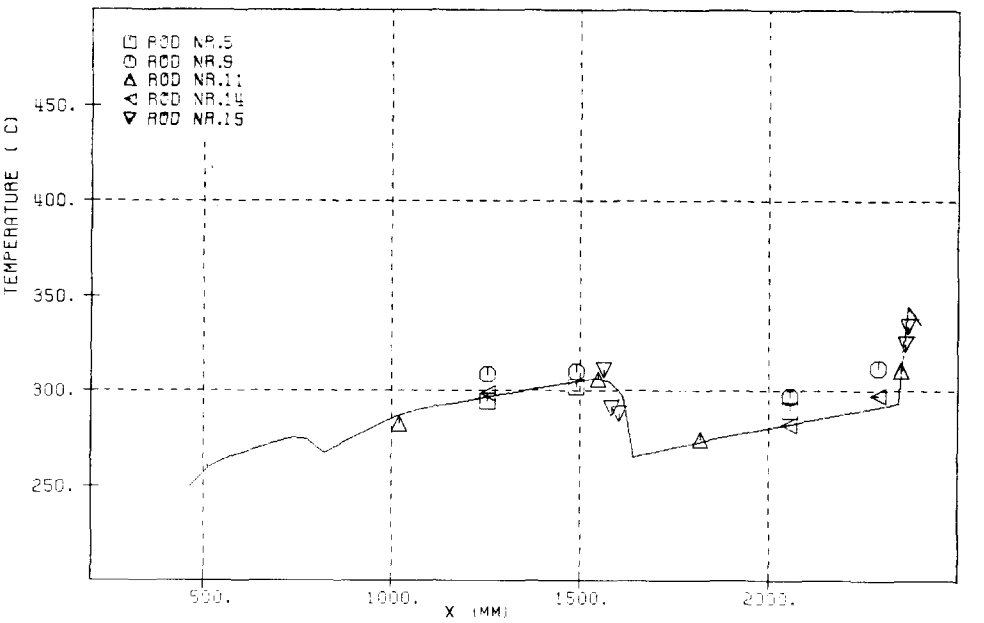

FIG. 14. Comparison between calculated and measured rod temperatures in the central subchannels relative to the outer row of rods (different position of the thermocouples from that of Fig. 13, 19-rod bundle, turbulent flow: $Re_E = 1.12 \times 10^5$).

the Nusselt numbers relative to the smooth walls has been assumed to be $(T_W/T_E)^{-0.2}$ according to [9]. since the coolant is helium.

All the figures show clearly the inlet effect on the rod temperatures. The computed temperature profiles are shown from about one equivalent diameter after the beginning of the heating, at the point where the Petukhov–Roizen equations [8] start to be valid. The effect of the first spacer on the pin temperature is also evident. After the influence of this spacer has vanished, the rod temperatures increase linearly, up to the end of the smooth portion. At the beginning of the roughened portion, the rod wall temperature decreases abruptly due to the considerable increase of the heat transfer coefficient owing to the roughness. The effect of the second spacer cannot be noticed because this spacer is near the end of the

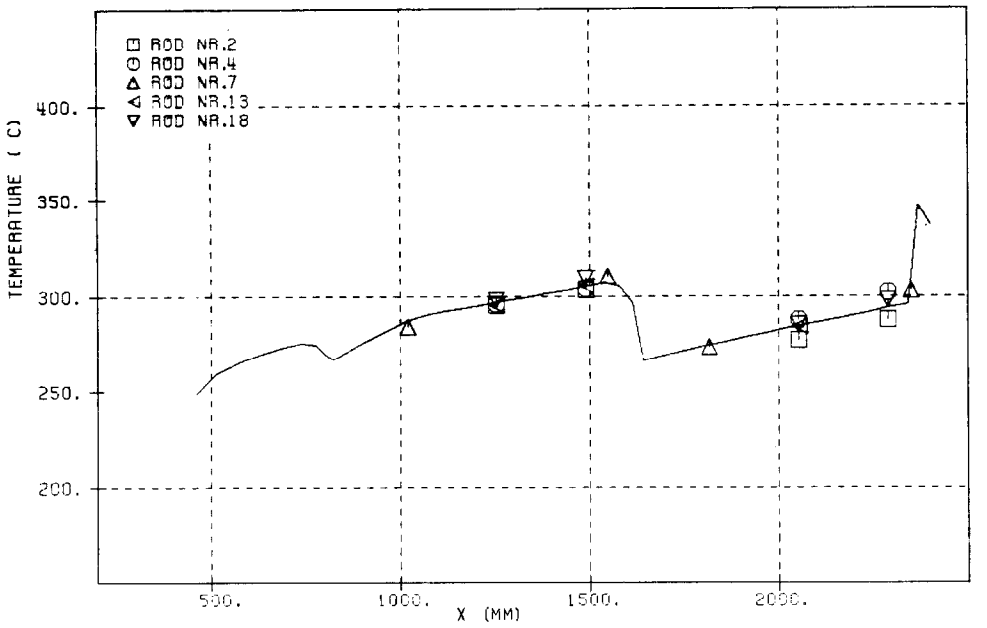

FIG. 15. Comparison between calculated and measured rod temperatures in the central subchannels relative to the outer row of rods (different position of the thermocouples from those of the previous Figs. 13 and 14, 19-rod bundle, turbulent flow: $Re_E = 1.12 \times 10^5$).

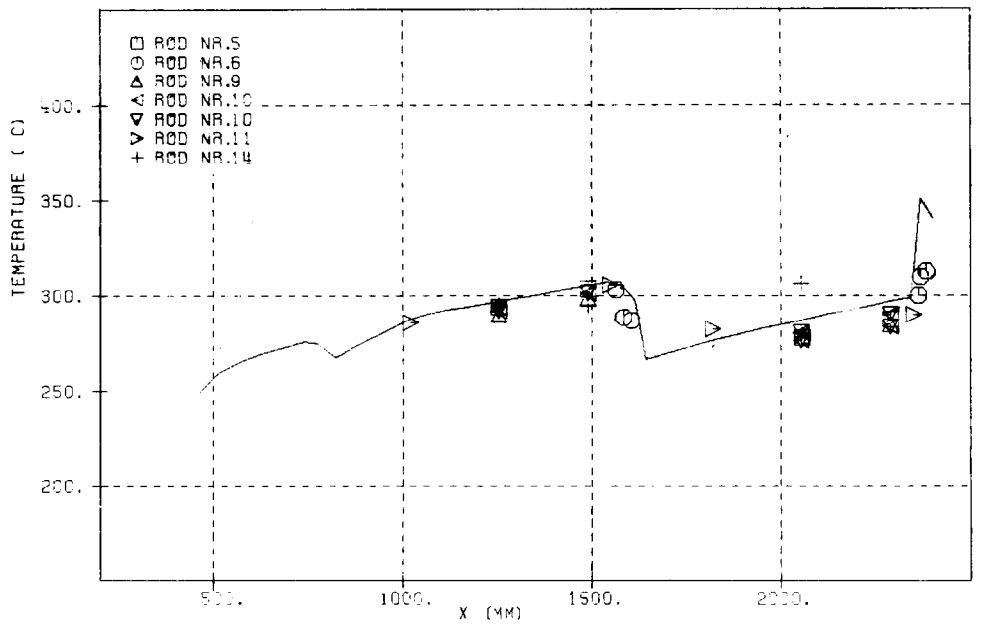

FIG. 16. Comparison between calculated and measured rod temperatures in the central subchannels relative to the inner row of rods (19-rod bundle, turbulent flow: $Re_E = 1.12 \times 10^5$).

axial smooth portion of the rods. At the end of the roughened portion there is a small heated smooth axial section, thus the rod temperatures increase suddenly. This temperature increase is observed in the measurements as well (see Fig. 14). The computed rod temperatures decrease then again, due to the effect of the third spacer. Figures 10–12 show also a comparison between the computed and measured shroud temperatures.

No equations were available to take into account the inlet effect on the shroud temperatures, thus the shroud temperature was assumed to be equal to the inlet temperature up to the axial position at which the value computed using the equation valid in case of fully developed flow was higher than the inlet temperature. Furthermore, no spacer effects on shroud temperature were taken into account, again due to the lack of equations. The

temperature of the shroud walls facing rough portions of the rods are higher than those of the shroud walls facing smooth portions of the rods, because the temperature profiles in the coolant subchannels confined by the rough heat transfer surfaces are flatter than those for channels surrounded by smooth surfaces only.

Considering the scattering of the experimental results, the agreement between calculations and measurements is good both for the rod and the shroud temperatures.

3.2. *Comparison between computed and experimental results for the* 12-*rod bundle*

The experiments were performed in the Reynolds number range $Re_E = 7 \times 10^3$ to $Re_E = 8 \times 10^4$. The maximum rod linear power achieved was 460 W cm^{-1}, resulting in a maximum heat flux of 185 W cm^{-2}. The maximum measured wall temperature was 790°C. Some of the directly measured experimental data are given in [28].

A comparison between computed and measured pressure losses, and rod and shroud temperatures for a thermal test for the 12-rod bundle at $Re_E = 5.45 \times 10^4$ (test 3 for CEIII)† has already been shown [4]. More precise measurements of the shroud dimensions have shown that the distance between the center of the external rods and the shroud wall is a little larger than the nominal value assumed in [4] (6.03 mm instead of 6.0 mm) and that the height of the "blocking triangles" is a little smaller (1.54 mm instead of 1.57 mm). This means larger external coolant channels. As it has been noticed that small variations of the flow section parameters give origin to considerable changes in the rod temperatures [4], the calculations for test 3 have been repeated.

Furthermore in these calculations, the pressure drop at the spacer grids is computed by means of the modified drag coefficients c_v obtained by measurements of the pressure drop of the grid of CEIII in the shroud of CEI [29]‡ carried out in the water loop of the Institute of Neutron Physics and Reactor Engineering, and transforming them to take account of the different values of the blockage factors of the spacers in the two shrouds. The c_v values obtained in this way are higher than those used in the calculations of [4], which were directly obtained from the measurements performed with helium in the test section CEIII. This is probably due to the fact that, evaluating the c_v values with the mentioned procedure, the influence of other important parameters beside the grid blockage factor, like the ratio between the wetted perimeters inside and outside the spacer region and especially the axial profile of the flow section inside the spacers, is neglected. In fact there is no concrete reason to have doubts about the clear tendency shown by the measurements in helium. Moreover, as pointed out in [4], the shroud walls of test section CEIII were clearly rough, due to the presence of some small bolts fixing the two halves of the shroud together (the effects of the shroud roughness had been taken into account in [4]). But a good agreement between computed and experimental pressure drop is found, in these latter calculations with c_v values measured in water, only assuming smooth shroud walls.

Furthermore, in the present calculations, in order to try to establish more accurately the mass-flow redistribution due to the spacers, we decided to use the correlation suggested by Jung and Böhner for evaluating the spacer pressure drop in the single subchannels [30], which was based on the cited measurements performed in water and reported in [29]. This correlation is more detailed and probably better than that suggested in [16] (where the function $c_v = c_v(Re)$ is assumed to be the same for all subchannels, also in case of spacers placed in the rough portion of the bundle); in fact at least it takes into account the fact that for rough rods, due to the larger friction inside the spacers (see [28, 29]), the c_v values are higher in the central channels than in the external ones, because all surfaces bounding the central channels with the exception of the grid walls themselves are roughened, while the walls bounding external channels are partly smooth.

According to [30] the spacer pressure loss [cf. equation (16)] is computed with the equation:

$$c_v = 6.82K'(1 + 891 \cdot Re^{-0.8135}) + 10.7(1 - K')(1 + 6026Re^{-1.104}), \quad (17)$$

where, for the spacers in the axial smooth portion of the rods:

$$K' = 1, \quad (18)$$

and for the spacers in the axial rough portion of the rods:

$$K' = \begin{cases} 0.2747 & \text{for the whole bundle flow section} \\ 0 & \text{for the central channels} \\ 0.366 & \text{for the wall channels} \\ 0.575 & \text{for the corner channels.} \end{cases} \quad (19)$$

Anyway, in spite of the above mentioned assumptions made for the present calculations, with respect to those of [4], no considerable differences in the computed mass flow and temperature distributions have been obtained, as can be seen from a comparison of the presently calculated temperatures of shroud and rods and the corresponding ones shown in [4].

For the calculations of the friction and heat transfer coefficients for the rough surfaces of the 12-rod bundle, the $R(h^+)$ and $G(h^+)$ were given again by the general correlation of Dalle Donne and

†For an explanation of the names of the different 12-rod bundle test sections see [4].

‡The shroud of CEI has been used for the measurements, because the CEIII bundle was needed for further experiments and, thus, could not be disassembled. These measurements were not available yet at the time of the calculations of [4].

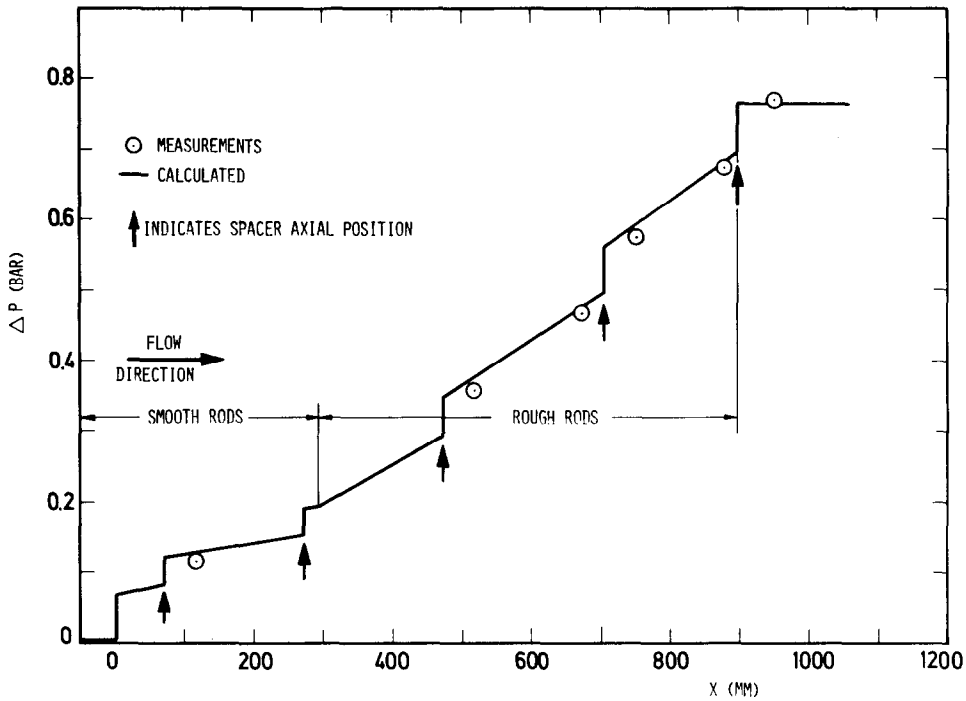

FIG. 17. Comparison between calculated and measured pressure drop in the 12-rod bundle by turbulent flow (turbulent flow: $Re_F = 5.45 \times 10^4$).

Meyer for two-dimensional rectangular ribs [26]:

$$R(h^+) = R(h_W^+)_{01} + 0.4 \ln\left(\frac{h}{0.01(r_0 - r_1)}\right) + \frac{5}{\sqrt{h_W^+}}\left(\frac{T_{W\infty}}{T_b} - 1\right)^2 \quad (20)$$

$$G(h^+) = g_0(h^+) Pr^{0.44}\left(\frac{T_{W\infty}}{T_B}\right)^{0.5} \times \left(\frac{h}{0.01(r_2 - r_1)}\right)^{0.053} \quad (21)$$

Originally the asymptotic value of $R(h_W^+)_{01}$, $R(h_W^+)_{01\infty}$, was taken equal to 4.3. This value is obtained from the Dalle Donne and Meyer correlation [26] assuming that the trapezoidal roughness ribs on the rods can be considered equivalent to rectangular ribs with their average width. However experiments performed in the Institute of Neutron Physics and Reactor Engineering with one of the rods of the 12-rod bundle inside a smooth tube, have shown that the $R(h^+)_{01\infty}$ values are slightly higher than 4.3, i.e. 4.7 [31]. This is probably due to the fact that the equivalence between trapezoidal and rectangular ribs is only approximate. In [4] the value of $R(h_W^+)_{01}$ used in the calculations was:

$$R(h_W^+)_{01} = 4.7 + \frac{359}{(h_W^+)^2}, \quad (22)$$

based on some preliminary isothermal tests of [31]. However the subsequent tests with heat transfer have shown that $R(h_W^+)_{01}$ remains more or less constant down to low values of h_W^+, thus the constant value:

$$R(h_W^+)_{01} = R(h_W^+)_{01\infty} = 4.7, \quad (23)$$

was used in the present calculations with equation (20).

According to [26], from the value $R(h_W^+)_{01\infty} = 4.7$ the following equation was established for the function $g_0(h^+)$ of equation (21) and used in the calculations:

$$g_0(h^+) = \begin{cases} g_1 = 4.4(h_W^+)^{0.24} & \text{if } g_1 \geq 10 \\ 10 & \text{if } g_1 < 10. \end{cases} \quad (24)$$

As for the 19-rod bundle, further assumptions for the calculations were uniform mass flow and temperature distributions at the bundle inlet, and no pressure recovery at the bundle outlet.

Figure 17 shows a comparison between computed and measured pressure drops for the test 3 here considered. As for the 19-rod bundle, the coefficient K_E for the inlet pressure loss (cf. equation (15)) was assumed equal to 1.2. The agreement between calculation and measurement is excellent (maximum discrepancy 3%), although some doubts remain, as already pointed out, about the c_v values given by the equations (17)–(19) and the assumption of smooth shroud walls. Figures 18–21 show the comparison between the computed and the measured rod temperatures in the various subchannels. In the ordinate axis of the diagrams $T_W + K$ is plotted, where T_W is the real rod temperature and K a fictitious temperature increment which allows a comparison of results for similar cases in the same plot. Due to the considerably higher heat fluxes at the rough rod walls and therefore higher Biot numbers than in the case of the 19-rod bundle, the fin efficiency effect is not negligible for the 12-rod bundle. The surface rod temperatures were thus

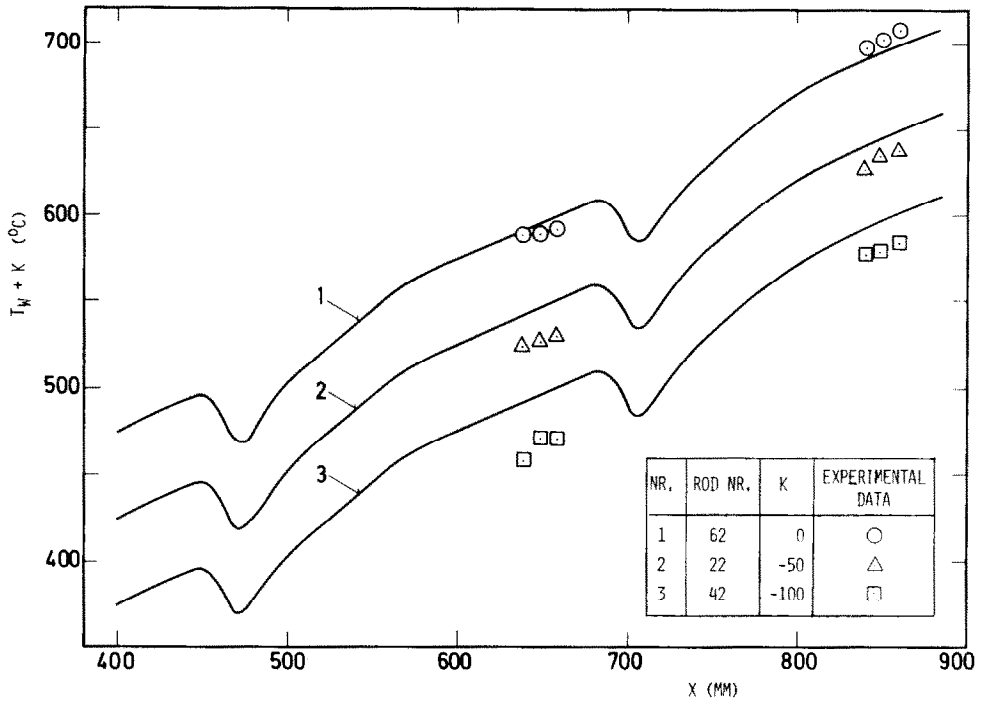

FIG. 18. Comparison between calculated and measured rod wall temperatures relative to the central channels (12-rod bundle, turbulent flow: $Re_E = 5.45 \times 10^4$, rough portion of the rods only).

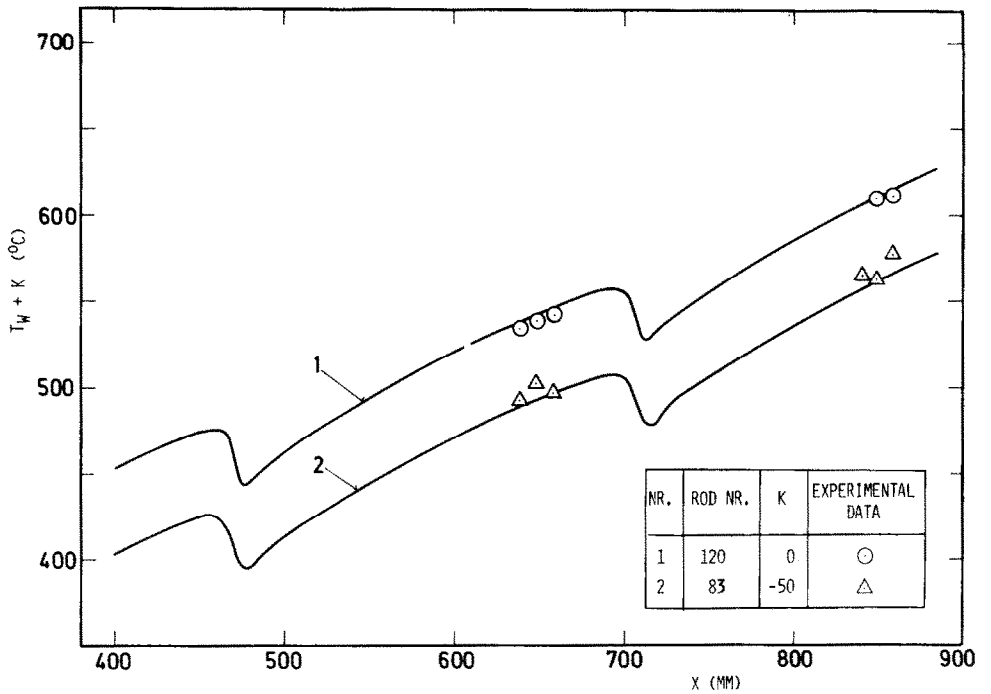

FIG. 19. Comparison between calculated and measured rod wall temperatures relative to the wall subchannels with 1/2 standoff of the spacer grid (12-rod bundle, turbulent flow: $Re_E = 5.45 \times 10^4$, rough portion of the rods only).

corrected by means of the parameter K_∞, with

$$K_\infty = 1 - 1.2B_i, \tag{25}$$

according to the correlation suggested in [22], which refers to roughness ribs very similar to those on the surface of the rods of the 12-rod bundle. As the thermocouples are set midway in the canning width, another correction was performed to evaluate the rod temperatures at this position, using equation (10). In the case of the 12-rod bundles even this correction cannot be neglected. In all the figures the spacer effect on the computed rod temperatures is

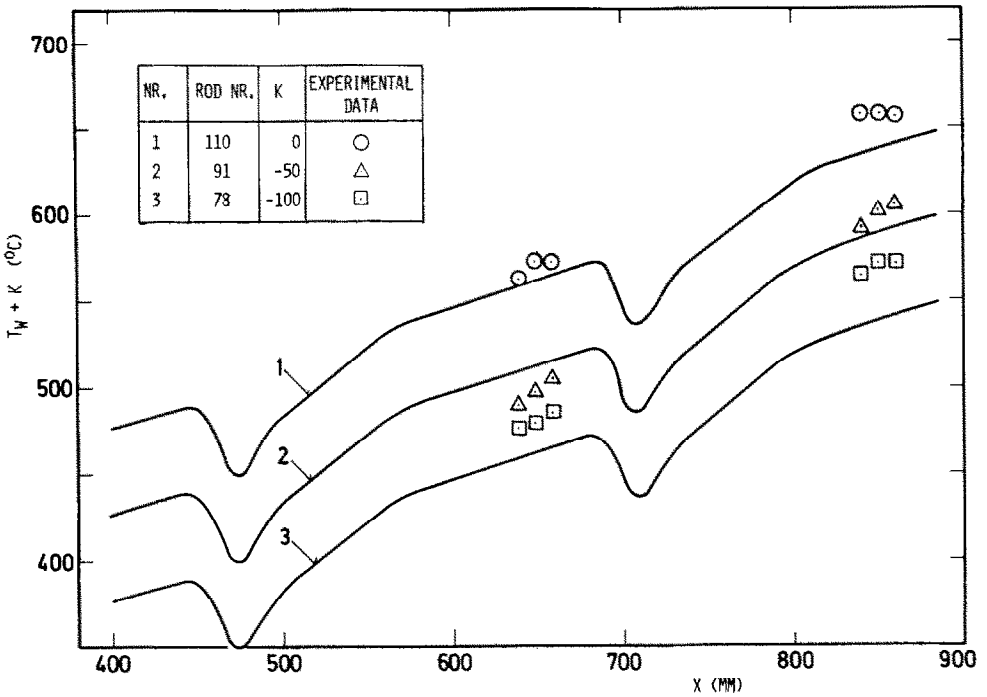

FIG. 20. Comparison between calculated and measured rod wall temperatures relative to the wall subchannels with one standoff of the spacer grid (12-rod bundle, turbulent flow: $Re_E = 5.45 \times 10^4$, rough portion of the rods only).

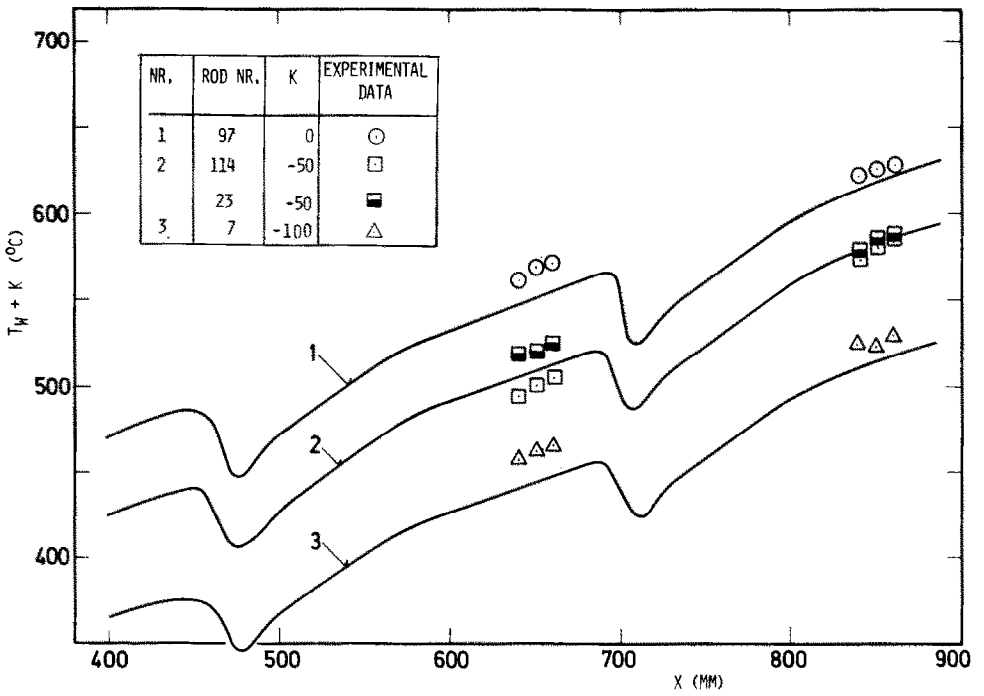

FIG. 21. Comparison between calculated and measured rod wall temperatures at the gaps between external channels (12-rod bundle, turbulent flow: $Re_E = 5.45 \times 10^4$, rough portion of the rods only).

evident. No inlet effect on the rod temperatures could be taken into account because of lack of correlations. Nevertheless the agreement between computed and measured rod temperatures is good. In fact the maximum differences are normally less than $\pm 20°C$ (i.e. less than 10% of the film drop) often being less than $\pm 10°C$ and only in one case being 30°C.†

†As shown by Figs. 18–21 the scattering of the experimental points is of approximately the same order of magnitude.

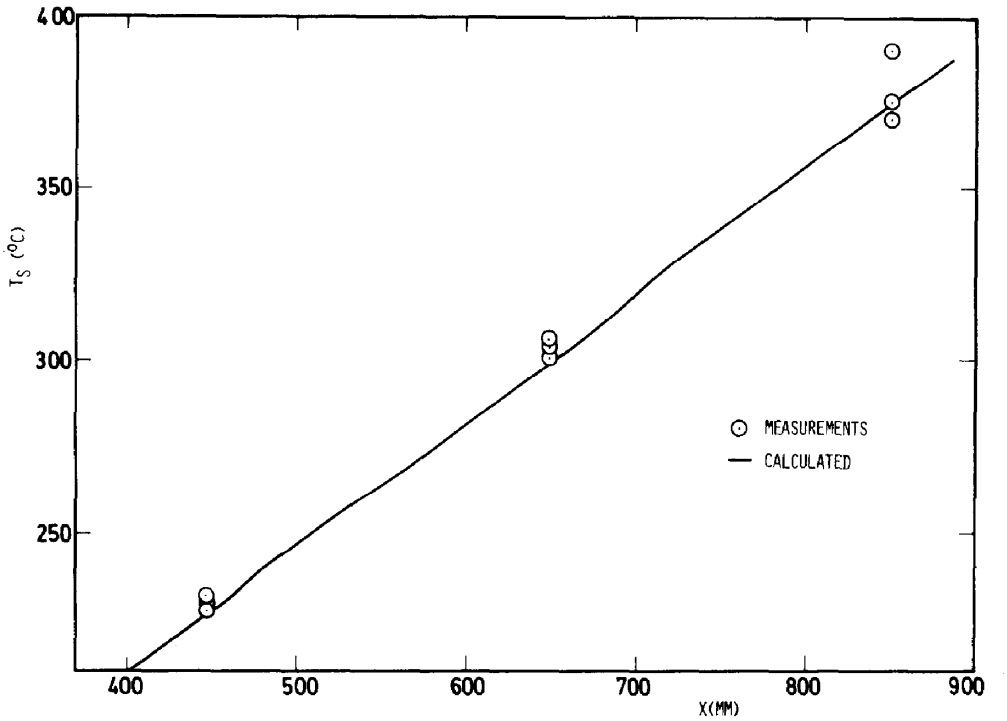

FIG. 22. Comparison between calculated and measured temperatures of the shroud wall (12-rod bundle, turbulent flow: $Re_E = 5.45 \times 10^4$, relative to the rough portion of the rods only).

Figure 22 shows the comparison for computed and measured shroud temperatures. As for the 19-rod bundles, where the first heated portion was smooth, the shroud temperature is assumed to be equal to the inlet gas temperature up to the axial position at which the value computed by means of the equation valid in the case of fully developed flow [6]:

$$T_{W_s} = T_{W\infty} - \frac{q}{\rho_B c_{PB} u_b^*}\left(2.5 \ln \frac{r_2 - r_1}{h} + G(h^+)\right), \quad (26)$$

becomes higher than the inlet temperature. Again the computed and measured temperatures agree well. It is worth pointing out that, the shroud wall temperature being computed as the gas temperature in the immediate vicinity of the shroud wall, equation (26) stems from the direct application of the logarithmic temperature profile (cf. equation (2)) and the good agreement between experimental and computed shroud temperatures is again a proof of the applicability of the logarithmic universal laws of the wall to the case of turbulent flow in a bundle of rough rods.

4. CONCLUSIONS

The good agreement between measurements and SAGAPØ calculations for two so different bundles as the 19- and 12-rod bundle leads to the following conclusions:

(a) The method of integrating the logarithmic velocity and temperature profiles in turbulent flow in the various coolant subchannels of the bundle to obtain the friction and heat transfer coefficients of the subchannels is not only more satisfactory theoretically than the direct use of the integral values friction factor, Stanton number and equivalent hydraulic diameter,† but leads to good results as well;

(b) The computer code SAGAPØ is a good tool to predict the wall temperature and the pressure drop of gas cooled rough rod bundles, at least for turbulent flow conditions. Due to this the SAGAPØ code has been already used for the heat transfer design of the 12-rod fuel element bundle to be irradiated in the BR2 reactor (Mol Experiment) [4]. SAGAPØ has also been successfully applied to different Benchmark problems in the frame of the GCFR collaboration (for example for a CO_2-cooled 37 rod-bundle tested at EIR [33]);

(c) SAGAPØ can calculate laminar flow as well. However agreement with experiment is not as good as for turbulent flow [23]. This is partly due to the fact that experimental errors increase with low flows and high temperatures, but also because SAGAPØ does not yet make allowance for conduction in the rods and heat transfer by thermal radiation which play an important role by low flows. The introduction of these two effects is under way.

†For instance Walker, White and Burnett were forced to use for each coolant channel of different form a different empirical equation for f and St to correlate their experimental data for a rough rod bundle [32].

Acknowledgements—We wish to thank Messrs. J. Marek, E. Mensinger, A. Roth and G. Wörner for their help in performing the experiments and some of the calculations.

REFERENCES

1. A. Martelli, Thermo- und fluiddynamische Analyse von gasgekühlten Brennelementbündeln, Kernforschungszentrum Karlsruhe Report KfK 2436, EUR 5508d (März 1977).
2. A. Martelli, SAGAPØ. A computer code for the thermo-fluid-dynamic analysis of gas cooled fuel element bundles, Kernforschungszentrum Karlsruhe Report KfK-2483, EUR 5510e (August 1977).
3. A. Martelli, SAGAPØ-2. An improved version of the SAGAPØ code for the thermo-fluid-dynamic analysis of gas cooled fuel element bundles, Kernforschungszentrum Karlsruhe Report KfK-2663, EUR 5753e (August 1978).
4. M. Dalle Donne, J. Marek, A. Martelli and K. Rehme, BR2 bundle mockup heat transfer experiments, *Nucl. Engng Design* **40**, 143–156 (1977).
5. A. Martelli and K. Rehme, Vergleich von Rechnungen und Messungen des Wärmeübergangs in einem gasgekühlten Stabbündel, Reaktortagung, Mannheim 29 März–1 April 1977, 19–22, Deutsches Atomforum E.V. (DAtF) (1977).
6. M. Dalle Donne, Wärmeübergang von rauhen Oberflächen, Kernforschungszentrum Karlsruhe Report KfK 2397, EUR 5506d (Januar 1977).
7. S. Nikuradse, Gesetzmäßigkeiten der turbulenten Strömung in glatten Rohren, *VDI Forschungsheft* 356 (1932).
8. B. S. Petukhov and L. I. Roizen, Generalized dependences for heat transfer in tubes of annular cross-section, *High Temp.* **12**, 485 (1975).
9. M. Dalle Donne and E. Meerwald, Heat transfer and friction coefficients for turbulent flow of air in smooth annuli at high temperatures, *Int. J. Heat Mass Transfer* **16**, 787–809 (1973).
10. K. Rehme, Laminarströmung in Stabbündeln, *Chem.-Ing.-Techn.* **17**, 962–966 (1971).
11. R. K. Shaw and A. L. London, Laminar flow convection heat transfer and flow friction in straight and curved ducts. A summary of analytical solutions. Technical Report No. 75, Mechanical Engineering Department, Stanford University, Stanford, California (1971).
12. R. A. Axford, Two-dimensional, multiregion analysis of temperature fields in reactor tube bundles, *Nucl. Engng Design* **6**, 25–42 (1967).
13. B. Kjellström, Studies of turbulent flow in triangular array rod bundles, A.B.Atomenergi Studsvik Report AE-487 (1974).
14. L. Ingesson and S. Hedberg, Heat transfer between subchannels in a rod bundle, Heat Transfer Conference, Paris, Vol. III, FC7.11 (1970).
15. U. Stiefel, Eidg. Institut für Reaktorforschung: Personal communication (1976).
16. K. Rehme, Pressure drop correlations for fuel element spacers, *Nucl. Technol.* **17**, 15–23 (1973).
17. J. Marek and K. Rehme, Experimentelle Untersuchung der Temperaturverteilung unter Abstandshaltern in glatten und rauhen Stabbündeln, Kernforschungszentrum Karlsruhe Report KfK 2128 (1975).
18. E. M. Sparrow and S. H. Lin, The developing laminar flow and pressure drop in the entrance region of annular ducts, *J. basic Engng* 827–834 (1964).
19. R. E. Lundberg, P. A. McCuen and W. C. Reynolds, Heat transfer in annular passages. Hydrodynamically developed laminar flow with arbitrarily prescribed wall temperatures or heat fluxes, *Int. J. Heat Mass Transfer* **6**, 495–529 (1963).
20. P. L. Mantle, A. R. Freemann and J. Watts, Conductivity effects on ribbed surface heat transfer, *Int. J. Heat Mass Transfer* **14**, 1825 (1971).
21. J. Watts, Effect of rib shape and spacing on conductivity corrections to ribbed surface heat transfer data, CEGB Report RD/B/N 2106 (1971).
22. M. Hudina and S. Yanar, The influence of heat conduction on the heat transfer performance of some ribbed surface tested in ROHAN experiment, EIR Report TM-IN-572 (1972).
23. A. Martelli, K. Rehme and F. Vannucci, Comparison between measured and calculated pressure and temperature distributions in a roughened rod bundle of 19-rods, OECD-NEA Coordinating Group on Gas Cooled Fast Reactor Development, 4th Specialist Meeting on GCFR Heat Transfer, Karlsruhe (1977).
24. K. Rehme, Experimentelle thermo- und fluiddynamische Untersuchungen an einem 19-Stabbündel mit künstlichen Oberflächenrauhigkeiten, Kernforschungszentrum Karlsruhe Report KfK 2313 (1976).
25. L. Meyer and K. Rehme, Verwendete Meßtechniken bei der Simulation der Thermo- und Fluiddynamik in Stabbündeln für Gasbrüter, 2.KTG-Fachtagung der Fachgruppe Thermo- und Fluiddynamik der KTG im DAtF über Experimentiertechnik auf dem Gebiet der Reaktorthermodynamik, Hannover (28 Februar–2 März 1977).
26. M. Dalle Donne and L. Meyer, Turbulent convective heat transfer from rough surfaces with two-dimensional rectangular ribs, *Int. J. Heat Mass Transfer* **20**, 583–620 (1977).
27. M. Dalle Donne and L. Meyer, Convective heat transfer from rough surfaces with two-dimensional ribs: transitional and laminar flow, Kernforschungszentrum Karlsruhe Report KfK 2566, EUR 5751e (January 1978).
28. K. Rehme, Auswertung der fluiddynamischen Untersuchungen an einem Stabbündel mit 12 Stäben (Mol-Kalibrierelement), in *1. Vierteljahresbericht 1976*, Projekt Schneller Brüter, Kernforschungszentrum Karlsruhe Report KfK 1276/1, pp. 127–1 (Juli 1976).
29. K. Rehme, Pressure drop of spacer grids in smooth and roughened rod bundles, *Nucl. Technol.* **33**, 314–317 (1977).
30. W. Jung and G. Böhner, Kraftwerk Union, Erlangen: Private communication (1977).
31. M. Dalle Donne and L. Meyer, Kernforschungszentrum Karlsruhe. Unpublished (1978).
32. V. Walker, L. White and P. Burnett, Forced convection heat transfer for parallel flow through a roughened rod cluster, *Int. J. Heat Mass Transfer* **15**, 403–424 (1972).
33. M. Hudina, P. Barroyer and M. Huggenberger, Eidg. Institut für Reaktorforschung, Würenlingen, Switzerland. Unpublished (1977).

EXPERIENCES THERMO ET AEROHYDRODYNAMIQUES SUR DES FAISCEAUX D'AIGUILLES RUGUEUSES, REFROIDIS PAR GAZ, ET INTERPRETATION A L'AIDE DU PROGRAMME DE CALCUL SAGAPØ

Résumé—On décrit brièvement des expériences relatives au transfert thermique, effectuées sur un banc d'essai à hélium à haute pression avec deux faisceaux de 12 et de 19 aiguilles respectivement, chauffées électriquement. On présente les bases du programme de calcul SAGAPØ. SAGAPØ calcule les coefficients de frottement et de transfert de la chaleur pour un écoulement turbulent en intégrant les lois à la paroi pour la vitesse et la température dans les différents canaux de refroidissement pour des surfaces rugueuses. En outre, le mélange turbulent et l'écoulement transversal entre les canaux, les effets des espaceurs sur les températures de paroi et la perte de pression, le rendement des nervures des rugosités ainsi que les effets d'entrée sur les températures de paroi pour des surfaces lisses sont pris en compte. L'écoulement laminaire peut également être calculé. L'accord entre les données calculées et mesurées est excellent. Deux autres effets, à savoir la conduction thermique circonférentielle dans les aiguilles et le rayonnement ont été négligés jusqu'à présent; ces effets ne jouent un rôle important que pour de petites vitesses d'écoulement et des températures élevées.

THERMO- UND FLUIDDYNAMISCHE EXPERIMENTE AN GASGEKÜHLTEN, RAUHEN STABBÜNDELN UND DEREN AUSWERTUNG MIT DEM RECHENPROGRAMM SAGAPØ

Zusammenfassung—Experimente zum Wärmeübergang in einem Hochdruck-Heliumversuchsstand mit zwei Stabbündeln mit 12 bzw. 19 elektrisch beheizten, rauhen Stäben werden kurz beschrieben. Die Grundlagen des SAGAPØ Rechenprogramms werden dargelegt. SAGAPØ berechnet die Reibungsbeiwerte und Wärmeübergangs koeffizienten für turbulente Strömung durch Integration der universellen logarithmischen Wandgesetze für Geschwindigkeit und Temperatur in den verschiedenen Kühlkanälen bei rauhen Oberflächen. Außerdem werden turbulente Vermischung und Querströmung zwischen den Kanälen, Auswirkungen der Abstandshalter auf Wandtemperaturen und Druckverlust, der Rippenwirkungsgrad der Rauhigkeiten sowie Eintrittseffekte auf die Wandtemperaturen bei glatten Oberflächen berücksichtigt. Laminarströmung kann ebenfalls berechnet werden. Die Übereinstimmung zwischen berechneten und gemessenen Daten ist für turbulente Strömung sehr gut. Zwei weitere Effekte, nämlich die Wärmeleitung in Umfangsrichtung in den Stäben sowie die Wärmestrahlung werden bisher vernachlässigt; diese Effekte spielen nur bei kleinen Strömungsgeschwindigkeiten und hohen Temperaturen eine bedeutende Rolle.

ЭКСПЕРИМЕНТАЛЬНЫЕ ТЕРМОГИДРОДИНАМИЧЕСКИЕ ИССЛЕДОВАНИЯ ОХЛАЖДЕНИЯ ГАЗОМ ПУЧКОВ ШЕРОХОВАТЫХ СТЕРЖНЕЙ И ОБРАБОТКА РЕЗУЛЬТАТОВ НА ЭВМ С ПОМОЩЬЮ ПРОГРАММЫ САГАПО

Аннотация — Дано краткое описание экспериментов по теплообмену двух пучков из 12 и 19 шероховатых стержней, нагреваемых электрическим током и расположенных в гелиевом контуре с высоким давлением. Изложены основные принципы составления программы САГАПО. Данная программа используется для расчёта коэффициентов трения и теплопереноса в турбулентном потоке с помощью интегрирования логарифмического универсального закона стенки для скорости и температуры в различных охлаждающих каналах, ограниченных шероховатыми поверхностями. В программе учитываются турбулентное смешение и переток жидкости между каналами, влияние распорок на температуру стенок и перепад давления, эффективность шероховатости, а также влияние условий входа на температуру стенки для стержней с гладкой поверхностью. С помощью данной программы можно также провести расчёт ламинарного течения. Для турбулентного потока получено хорошее совпадение экспериментальных данных с результатами расчётов. В программе не учитываются передача тепла за счёт теплопроводности по окружности стержней и тепловое излучение. Эти эффекты играют важную роль при небольших скоростях потока и высоких значениях температуры.